International Journal of Biological Macromolecules 69 (2014) 353–360

Contents lists available at ScienceDirect

International Journal of Biological Macromolecules

journal homepage: www.elsevier.com/locate/ijbiomac

Equilibrium unfolding of cyclophilin from *Leishmania donovani*: Characterization of intermediate states

Sourav Roy[a,1], Sankar Basu[a,1], Alok K. Datta[b], Dhananjay Bhattacharyya[a,1], Rahul Banerjee[a,*], Dipak Dasgupta[a,*]

[a] Saha Institute of Nuclear Physics, 1/AF Bidhannagar, Kolkata 700064, West Bengal, India
[b] Indian Institute of Chemical Biology, 4, Raja S.C. Mullick Road, Kolkata 700032, West Bengal, India

ARTICLE INFO

Article history:
Received 7 March 2014
Received in revised form 20 May 2014
Accepted 24 May 2014
Available online 2 June 2014

Keywords:
Cyclophilin
Intermediate
Protein unfolding

ABSTRACT

Cyclophilin from *Leishmania donovani* (LdCyp) is a ubiquitous peptidyl-prolyl cis-trans isomerase involved in a host of important cellular activities, such as signaling, heat shock response, chaperone activity, mitochondrial pore maintenance and regulation of HIV-1 infectivity. It also acts as the prime cellular target for the auto-immune drug cyclosporine A (CsA). LdCyp is composed of a beta barrel encompassing the unique hydrophobic core of the molecule and is flanked by two helices (H1, H2) on either end of the barrel. The protein contains a lone partially exposed tryptophan. In the present work the equilibrium unfolding of LdCyp has been studied by fluorescence, circular dichroism and the non-coincidence of their respective C_m's, indicates a non-two state transition. This fact was further corroborated by binding studies of the protein with bis-ANS and the lack of an isochromatic point in far UV CD. The thermal stability of the possible intermediates was characterized by differential scanning calorimetry. Further, MD simulations performed at 310, 400 and 450 K exhibited the tendency of both helices to partially unwind and adopt non-native geometries with respect to the core, quite early in the unfolding process, in contrast to the relatively stable beta barrel.

1. Introduction

Leishmaniasis, a broad spectrum of diseases caused by *Leishmania* spp. is widely prevalent in third world countries, among the poorer sections of the populace. The appearance of strains resistant to drugs (pentavalent antimonials) [1], traditionally used as the first line of defense against the pathogen, stress the need to continue the search for alternative drug targets, as second line drugs are generally expensive and have reportedly severe side effects [2]. Cyclophilin from *Leishmania donovani* (LdCyp) belongs to the ubiquitous class of peptidyl-prolyl cis-trans isomerases (PPIases), also known to be the intracellular receptor of the immunosuppressive drug cyclosporine A (CsA), a cyclic undecapeptide constituted of non-natural amino acids. CsA derivatives formed by specific modification of its side chains have been shown to lack immunosuppressive activity though retaining its anti-trypanosomatid and anti-parasitic character [3,4]. In addition, cyclophilins have also been implicated in signal transduction, cell division, cell surface recognition, chaperone activity and heat shock response [5]. Other studies show Cyp's to be involved in the maintenance of mitochondrial transition pores [6] and regulation of HIV-1 infectivity by functional association with HIV-1 virions in humans [7].

Several crystal and NMR structures of CyPs in both ligated/unligated forms are currently available [8,9]. Cyclophilin (LdCyp) has been used as the model system in the present study. The three dimensional structure of LdCyp (2HAQ: 1.97 Å) [10] consists of an 8 stranded ß-barrel with two α helices located at either end. The location of the helices with respect to the barrel effectively blocks the solvent accessibility of the only hydrophobic core of the molecule, located in the interior of the barrel. The single domain molecule consists of a single cysteine residue and its enzymatic activity is hindered by the binding of CsA as there is considerable overlap between the native active site of the enzyme and the binding site for CsA, both being located on the face of the barrel. LdCyp consists of a single tryptophan (Trp 143 also involved in its active site) which is situated on a flexible 3_{10} helix (141–145) and is partially exposed to the solvent.

Given the intrinsic interest of Cyp's in general and specifically in *Leishmania*, LdCyp has been selected for unfolding studies, both thermally and with denaturant. There are reports of thermal

* Corresponding authors. Tel.: +91 33 2337 5345; fax: +91 33 2337 4637.
E-mail addresses: rahul.banerjee@saha.ac.in (R. Banerjee), dipak.dasgupta@saha.ac.in (D. Dasgupta).
[1] Tel.: +91 33 2337 5345; fax: +91 33 2337 4637.

http://dx.doi.org/10.1016/j.ijbiomac.2014.05.063
0141-8130/

denaturation studies on cyclophilin from mycobacterium tuberculosis both in the presence and absence of CsA. CsA binding did not appear to impart any extra stabilization to the protein, though facilitated the formation of secondary structural elements at lower temperatures (25 °C). The PPiA (cyclophilin A from *Mycobacterium tuberculosis*) tended to aggregate beyond 70 °C and unfolding induced via denaturant demonstrated that the loss in tertiary structure preceded the loss in secondary structure both in the presence and absence of CsA [11].

In the present study we probed the unfolding of LdCyp by guanidium chloride (GdmCl) by means of fluorescence, circular dichroism (CD), dynamic light scattering (DLS) spectroscopy and differential scanning calorimetry (DSC). The results from the studies indicate that most probably the unfolding of LdCyp proceeds via at least one equilibrium intermediate. We have made an attempt to structurally characterize this possible intermediate(s) using multiple spectroscopic tools and molecular dynamics simulations.

2. Materials and methods

2.1. Reagents and chemicals

Guanidium chloride (GdmCl), bis-anilino-8-napthalenesulphonate (bis-ANS) were obtained from Sigma–Aldrich (USA). Potassium dihydrogen orthophosphate (KH_2PO_4) and anhydrous dibasic potassium phosphate (K_2HPO_4) were purchased from Sisco Research Laboratories (SRL) and Nickel-nitrilotriacetic acid-agarose, superflow (Ni-NTA) from Qiagen (USA). All other chemicals used were of analytical grade.

2.2. Protein purification

As reported previously, residues 22–187 of LdCyp has been cloned into PQE32 (Qiagen) expression vector (with an additional 6x-His tag at the N-terminal), over expressed in M15 *Escherichia coli* cells and purified to homogeneity using a Ni-NTA column. The purified protein sample was dialyzed extensively against a buffer containing 0.02 M Tris (pH 8.5) and 0.02% NaN_3 and stored at 4 °C. Prior to all spectroscopic and calorimetric experiments the protein was extensively re-dialyzed in 25 mM potassium phosphate buffer (pH 7.5).

2.3. Fluorescence measurements

Intrinsic tryptophan fluorescence of the protein was measured at 25 °C on a Perkin Elmer LS55 spectrofluorimeter (Perkin Elmer Ltd., UK). LdCyp at 4 μM in 25 mM potassium phosphate buffer (pH 7.5) was excited at 295 nm and the emission spectra recorded in the range 310 nm to 450 nm with both excitation and emission slit widths of 5 nm. The spectra recorded at a scan speed of 200 nm/min were averaged over 4 scans. Appropriate controls for the background emission were subtracted in each case.

Fluorescence quenching of the lone tryptophan residue by neutral quenchers serves to indicate the degree of solvent exposure of the tryptophan residues in a protein. Quenching experiments with the neutral quencher acrylamide was performed for LdCyp (4 μM) pre-incubated with the denaturant. The acrylamide concentration in the protein sample was varied from (10 to 50 mM) and fluorescence spectra measured ranging from 310 to 450 nm, with excitation at 295 nm. Stern–Volmer quenching constant was calculated as the slope of the plot of F_0/F values at 360 nm against the input concentration of quencher, acrylamide in the Stern–Volmer equation:

$$\frac{F_0}{F} = 1 + K_{SV}[Q] \quad (1)$$

where K_{SV} is the Stern–Volmer constant and [Q] is the concentration of the quencher. All quenching experiments were repeated thrice.

Binding of hydrophobic fluorescent dye, bis-ANS (bis-anilino-8-napthalenesulphonate), with LdCyp was carried out to probe the intermediate conformational states of LdCyp (4 μM, 25 mM potassium phosphate buffer, pH 7.5) in varying concentrations of the denaturant (GdmCl, 0.0–3.0 M). The protein along with the denaturant was equilibrated with bis-ANS for 20 min before recording the spectra. Ensuring complete saturation of the dye binding sites in the native protein the concentration of bis-ANS in the samples was kept fixed at 10 μM. Bis-ANS emission spectra was recorded from 410 to 675 nm, with excitation at 395 nm and both emission and excitation slit widths were kept at 5 nm. Appropriate buffer corrections were done.

2.4. Circular dichroism measurements

The CD spectra of LdCyp were recorded on a JASCO J715 (Jasco Corporation, Tokyo, Japan) in a rectangular quartz cell of path length 1 mm. Far UV measurements of LdCyp were recorded in the wavelength range of 200–250 nm For all CD experiments in 200–250 nm region, spectra were obtained by averaging over 4 scans, utilizing a slit width of 1 nm. For protein unfolding with chemical denaturants far UV spectra were recorded from 210 to 250 nm in case of GdmCl concentrations exceeding 1.0 M. Near UV spectra were recorded in the region 250–300 nm to probe the denaturant induced alteration of tertiary structure of the protein. Buffer contributions alone or with denaturants were subtracted from all protein spectra.

The observed values (after appropriate buffer corrections) were converted to mean residue ellipticity (MRE) in deg cm^2 $dmol^{-1}$ defined as

$$\text{MRE} = \frac{M\theta_\lambda}{10dcr} \quad (2)$$

where M is the molecular weight of the protein (in Da), θ_λ is the CD in millidegree, d is the path length in cm, c is the protein concentration in mg/ml and r the number of amino acid residues in the protein polypeptide chain.

2.5. Differential scanning calorimetry

10 μM of LdCyp was scanned on a VP-DSC Microcalorimeter (Microcal LLC, Northampton, MA, USA) from 10 °C to 70 °C with a scan rate of 30 °C/h and at approximately 28 psi pressure. All samples were extensively degassed prior to loading. Initially, the buffer (25 mM potassium phosphate, pH 7.5) or buffer combined with denaturant (GdmCl, 0.2–1.4 M) were repeatedly scanned to ensure a stable baseline. The buffer baseline was subtracted from the protein thermogram using Microcal Origin version 7.0 provided with the instrument, subsequent to normalization of the data by the protein concentration a non-linear curve fitting algorithm was employed to obtain the thermodynamic parameters of the transition. The reversibility of unfolding was checked at different scan rates, buffer conditions and temperature ranges. All experiments were repeated at least three times.

2.6. Guanidium chloride (GdmCl) mediated unfolding

Equilibrium unfolding of LdCyp was induced by 16 h of incubation with varying concentrations of GdmCl (0.025–3.0 M) at 25 °C. For refolding experiments, the unfolded protein with 3.0 M GdmCl was extensively dialyzed for 3 h against separate buffers containing 2.0, 1.5, 1.0, 0.5, 0.2 M GdmCl and was subsequently equilibrated again for 2 h. Fluorescence and CD spectra under different

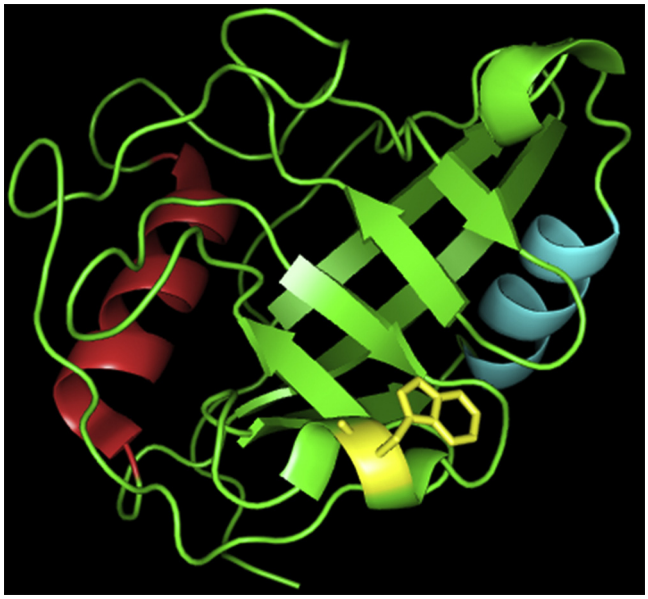

Fig. 1. Native crystal structure of cyclophilin from *Leishmania donovani* (LdCyp) in green (cartoon representation) with the partially solvent exposed lone tryptophan residue Trp 143 (in yellow, ball and stick mode). Helix H1 is colored red and helix H2 colored cyan. The figure is generated using Pymol.

conditions were then recorded as described above. The increase in GdmCl concentration in the buffer caused a negligible change in the pH of the solution.

2.7. Molecular dynamics simulations

Unfolding molecular dynamics simulations were performed on cyclophilin (coordinates obtained from: 2HAQ) at temperatures 310, 400 and 450 K. Each simulation run was for a duration of 50 ns. The simulation at 310 K could be considered to be 'native'. Initially, the protein was solvated in a cuboidal box of dimensions 78.683, 68.897 and 78.137 Å by the addition of 11,088 waters following the TIP3P model and charge neutralization of the system was accomplished by the addition of Na^+ ion utilizing the xleap module of AMBER [12]. The structure was then energy minimized (AMBER 2002 force field) for 200 steps of steepest descent followed by 19,800 steps of ABNR incorporated in the SANDER module. All simulations were performed using NAMD 2.0 [13]. For each 50 ns run the targeted temperature was attained in increments of 10 K/ps for a NPT ensemble with the Langevin piston set to the targeted temperature (310, 400, 450 K, etc.) and the pressure fixed at 1.032 bar. The bond lengths were constrained at a tolerance level of 0.005 Å by the SHAKE [14] algorithm. Visual molecular dynamics program (VMD 1.9.1) [15] was used to view the trajectories obtained from NAMD. The time step (δt) for the velocity–verlet algorithm was kept fixed at 1 fs. Snapshots were sampled at intervals of 10 ps. Secondary structural content for the snapshots were calculated using STRIDE [16].

3. Results and discussion

3.1. Unfolding of LdCyp with GdmCl

As mentioned previously, LdCyp contains a single tryptophan residue (Fig. 1). The maximum intensity of intrinsic fluorescence, λ_{max}, was observed at 348 nm for the native protein suggestive of the partial solvent exposure of the lone tryptophan. The emission spectrum changed with the variation of denaturant concentration till 1.4 M GdmCl. Further increase in the concentration of the

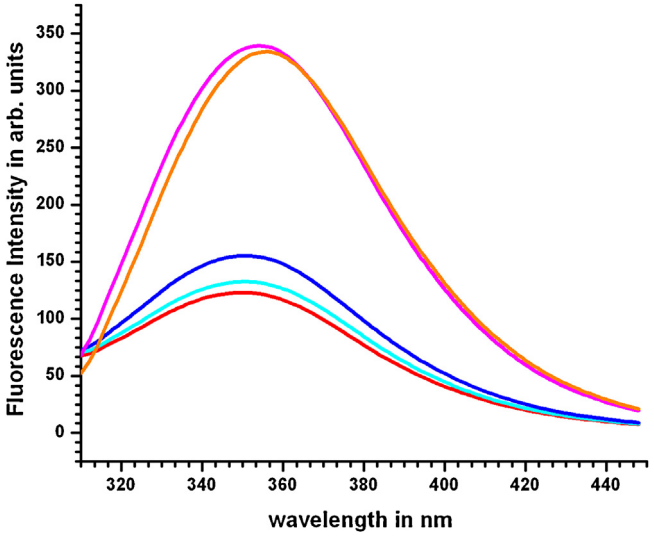

Fig. 2. Fluorescence unfolding spectra of native cyclophilin at various GdmCl concentrations ranging from (0 to 3) M. (a) ( ) 4 μM LdCyp, (b) ( ) 4 μM LdCyp + 0.8 M GdmCl, (c) ( ) 4 μM LdCyp + 1.0 M GdmCl, (d) ( ) 4 μM LdCyp + 1.4 M GdmCl, (e) ( ) 4 μM LdCyp + 3.0 M GdmCl.

denaturant led to a slight decrease in the intensity (Fig. 2). We plotted the intensity at 360 nm as a function of GdmCl concentration (Fig. 3). With increase in GdmCl concentration unfolding was initiated around 1.0 M and completed by 2.0 M, as clearly indicated by the saturation in fluorescence intensity.

The unfolding curve of LdCyp fitted best to a three state equation originating from the following equilibrium: $N \rightleftharpoons I \rightleftharpoons U$

$$S_{obs} = \frac{S_N + S_I e(-\Delta G_{NI}/RT) + S_U e(-\Delta G_{NU}/RT)}{1 + e(-\Delta G_{NI}/RT) + e(-\Delta G_{NU}/RT)} \quad (3)$$

where S_{obs} is the signal at any denaturant concentration, S_N is the signal due to the native state, S_I the signal due to the intermediate state and S_U the signal due to the unfolded state. ΔG_{NI} and ΔG_{NU} are the corresponding free energies of the transitions from $N \rightleftharpoons I$ and $N \rightleftharpoons U$ states [17] where ΔG_{NI} and ΔG_{NU} are assumed to have

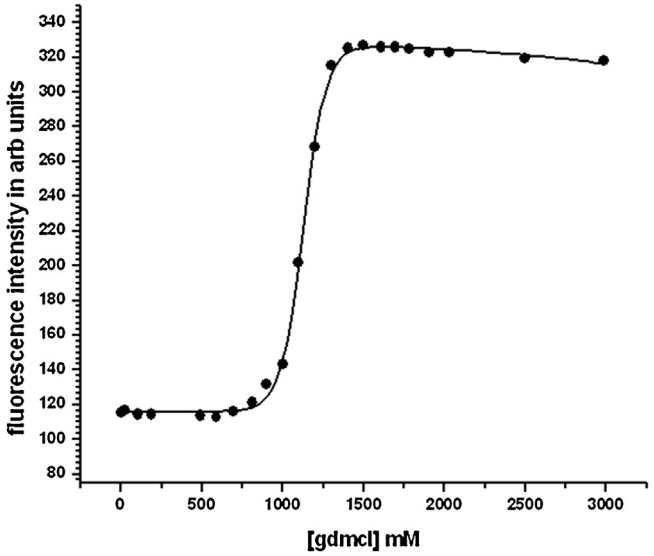

Fig. 3. Unfolding curve of LdCyp induced by GdmCl as monitored by intrinsic tryptophan fluorescence with emission maxima points at 360 nm, fitted to a 3-state equation. The black circles (•) indicate the fluorescence intensity in arbitrary units at the corresponding denaturant concentrations (in mM) and ( ) is the fitted line to the data points.

Table 1
Equilibrium thermodynamic parameters of unfolding for LdCyp mediated by GdmCl.

Spectroscopic tools employed	Thermodynamic parameters					
	$\Delta G_{NI}(H_2O)$ (kcal mol^{-1})	m_{NI} (kcal mol^{-1} M^{-1})	$\Delta G_{NU}(H_2O)$ (kcal mol^{-1})	m_{NU} (kcal mol^{-1} M^{-1})	$C_m(N \leftrightarrow I)$ (M)	$C_m(N \leftrightarrow U)$ (M)
Intrinsic tryptophan fluorescence	12.13 (±0.38)	−8.17 (±0.92)	6.72 (±0.54)	−5.89 (±0.65)	1.47 ± 0.06	1.16 ± 0.04
Far UV circular dichroism	2.12 (±0.13)	−2.18 (±0.29)	5.24 (±0.45)	−3.47 (±0.43)	0.99 ± 0.02	1.51 ± 0.04

The thermodynamic parameters in this table were obtained from the 3-state equation, Eq. (3) by employing a non-linear least square algorithm. $\Delta G_{NI}(H_2O)$ and $\Delta G_{NU}(H_2O)$ refers to the free energy of transition from the native to the intermediate state and native to the unfolded state, respectively, at zero denaturant concentration with ΔG_{NI} and ΔG_{NU} going to zero. m_{NI} and m_{NU} are the corresponding slopes of the transition from the native to the intermediate and native to the unfolded states, $C_m(N \leftrightarrow I)$ and $C_m(N \leftrightarrow U)$ are the midpoints of transition (denaturant concentration) obtained from Eqs. (4) and (5), where ΔG_{NI} and ΔG_{NU} goes to zero.

linear dependence with the denaturant concentration [D], resulting in the following equations,

$$\Delta G_{NI} = \Delta G_{NI}(H_2O) + m_{NI}[D] \quad (4)$$

$$\Delta G_{NU} = \Delta G_{NU}(H_2O) + m_{NU}[D] \quad (5)$$

where m_{NI} and m_{NU} are the corresponding slopes of transitions from the native to the intermediate and native to the unfolded states respectively. C_m for any unfolding curve is defined as the midpoint of the transition from the native to the unfolded state ($C_m(N \leftrightarrow U)$: for a 2-state transition) or between the native to intermediate and native to the unfolded state, respectively (that is $C_m(N \leftrightarrow I)$, $C_m(N \leftrightarrow U)$ for a three state transition) obtained from Eqs. (4) and (5) when the corresponding free energies of transition from the native to the intermediate state ΔG_{NI} and from the native to the unfolded state ΔG_{NU} becomes zero. The above fit yielded $\Delta G_{NI}(H_2O)$ of 12.13 kcal mol^{-1} with m_{NI} of −8.166 kcal mol^{-1} M^{-1} and $\Delta G_{NU}(H_2O)$ of 6.72 kcal mol^{-1} and m_{NU} of 5.89 kcal mol^{-1} M^{-1} (Table 1) which suggests that the unfolding of N to I exposes more solvent accessible surface area than the unfolding of N to U which is also clear from other experiments like (acrylamide quenching and bis-ANS fluorescence studies).

The far UV CD of the native protein exhibited a pronounced minimum at 225 nm characteristic of a protein with prevalently β-sheets. With the addition of GdmCl, MRE value at 222 nm progressively reduced from 0.8 to 2.0 M, saturating thereafter. This was also accompanied by a gradual and concomitant reduction in the overall secondary structural content till 1.2 M GdmCl, after which there was an abrupt loss of all secondary structural features in the protein (Fig. 4). Thus the CD signature of secondary structural feature was observed till 1.2 M GdmCl. Similar to the feature obtained from fluorescence titration profile (Fig. 3), the unfolding curve from CD value at 222 nm was best fitted to the above three state equation yielding ΔG_{NI} (H_2O) and C_m1 of 2.12 (±0.13) kcal mol^{-1} and 0.97 (±0.11) M and ΔG_{NU} (H_2O) of 5.24 (±0.16) kcal mol^{-1} and C_m2 of 1.51 (±0.2) M, respectively (Fig. 5). In addition, CD unfolding curves at MRE_{225} and MRE_{215} (Supplementary Information, Fig. S1 and Table S1a, S1b, S1c) gave similar C_m values though some deviation in the curves were observed between MRE_{222}, MRE_{225} on one hand and MRE_{215} on the other.

The lack of superposition of the unfolding curves obtained by two independent probes CD and fluorescence and the consequent non-equivalence of their respective C_m values (Table 1) appears to be supportive of a non-two state transition and thereby indicates the presence of a possible intermediate in the unfolding of LdCyp: N ⇌ I ⇌ U (see Supplementary Information, Fig. S2). There are numerous instances in the literature where non-coincidence of C_m values in equilibrium unfolding experiments [17–20] via two independent probes has been cited as evidence for the presence of an equilibrium intermediate. The adoption of a three state model improved the fitting in the protein unfolding curve monitored by fluorescence, when compared to a 2 state model (see

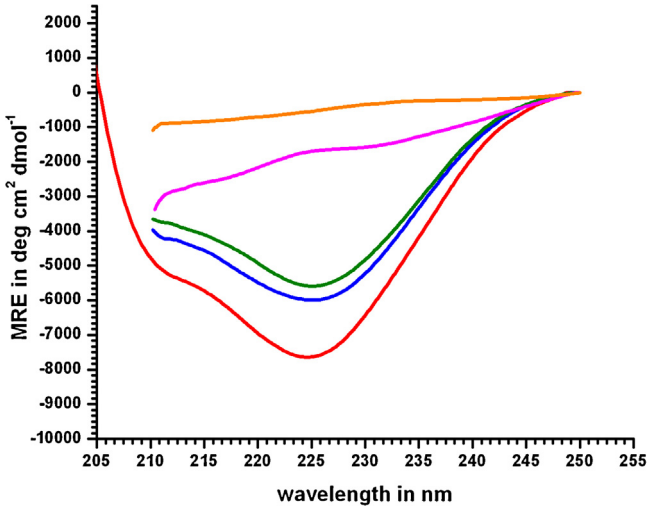

Fig. 4. Far-UV CD spectra of LdCyp (native) along with different denaturant concentrations. (a) ( ) 4 μM LdCyp (b) ( ) 4 μM LdCyp + 1 M GdmCl, (c) ( ) 4 μM LdCyp + 1.2 M GdmCl, (d) ( ) 4 μM LdCyp + 1.4 M GdmCl, (e) ( ) 4 μM LdCyp + 3.0 M GdmCl.

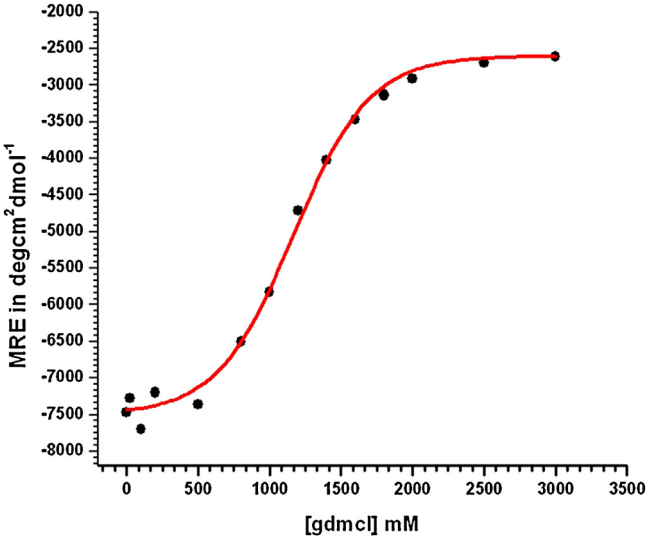

Fig. 5. MRE_{222} [in black circles (•)] values obtained from far-UV CD spectra plotted as a function of the denaturant and fitted to a 3-state equation.

Supplementary Information, Fig. S3). However, for unfolding curves monitored by CD (MRE_{222}) the improvement was only marginal (3-state compared to 2-state) (see Supplementary Information, Fig. S4). Notably, a 2-state transition could also be considered adequate in protein unfolding probed by CD. In any case for both fluorescence, CD the improved fitting (3-state versus 2-state) was only mildly reflected in their respective R^2 values. However, three state fittings were retained for both fluorescence and CD for consistency with bis-ANS fluorescence intensity (recorded at 488 nm) curves as function of GdmCl concentration and also because of the lack of an isochromatic point in the far UV CD data (ranging from 210 to 250 nm), generally indicative of a non-two state transition. Near UV CD (250–300 nm) spectra of native LdCyp show a broad shoulder in the region of 260–285 nm. CD spectra of LdCyp incubated with low concentration of GdmCl (0.2 M) indicate that the native tertiary interactions are relatively preserved. In contrast LdCyp incubated with 1.0 M and 1.2 M of GdmCl shows considerable perturbation in the native tertiary contacts as manifested by the reduced intensity of the broad shoulders (Fig. 6). Absence of tertiary interaction at high GdmCl concentration is evident from the featureless spectra with a significant reduction in band intensity. Summing up, the results from CD studies suggest that LdCyp thus incubated with 1.0 and 1.2 M of GdmCl shows considerable disruption in the original tertiary interactions whilst conserving their secondary structure.

To further characterize the intermediate hydrophobic dye binding studies with bis-ANS were performed.

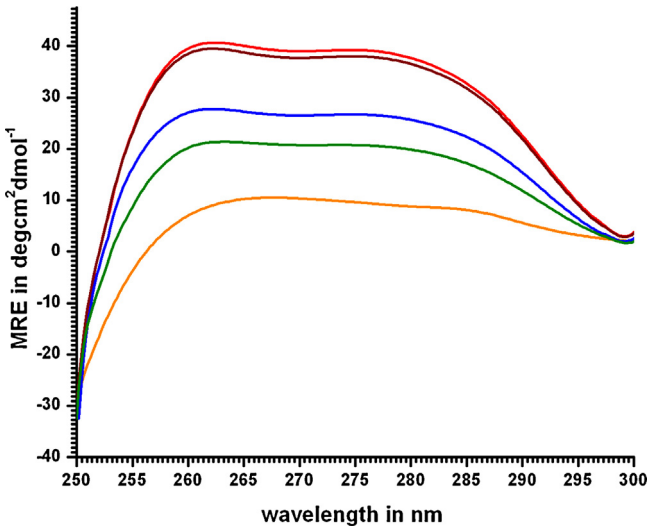

Fig. 6. Near UV CD spectra of LdCyp for (a) native protein LdCyp ( ) 40 μM, (b) LdCyp + 0.2 M GdmCl ( ) maintaining a characteristic broad shoulder which considerably flattens out for (c) LdCyp + 1.0 M GdmCl ( ), (d) LdCyp + 1.2 M GdmCl ( ), (e) LdCyp + 3.0 M GdmCl ( ), thereby depicting the loss of tertiary interactions with increasing denaturant concentrations.

3.2. Bis-ANS fluorescence experiment

Bis-ANS fluorescence studies have been widely used to identify intermediate states in protein unfolding [21,22]. Natively folded or completely unfolded proteins are unable to bind to bis-ANS, as their hydrophobic cores are effectively shielded in the former, whereas in the latter dissolution of the core negates any dye binding even though the hydrophobic residues are solvent exposed. Thus the partial exposure of erstwhile buried hydrophobic residues characteristic of "molten globules" are ideal for bis-ANS interaction. For LdCyp, bis-ANS fluorescence intensity (recorded at 488 nm) initially rose with GdmCl concentration upto 1.2 M and declined thereafter with a minima at 3.0 M (Figs. 7 and 8).

Both of these observations are indicative of a molten globule like intermediate in the equilibrium unfolding of LdCyp.

3.3. Acrylamide quenching

Stern–Volmer coefficients estimated for different denaturant concentrations (see Section 2.3) yielded a K_{SV} value of 7.64 M^{-1} for the native protein indicating partial solvent exposure of its lone tryptophan. K_{SV} increased to 13.18 M^{-1} at 1.4 M concentration of

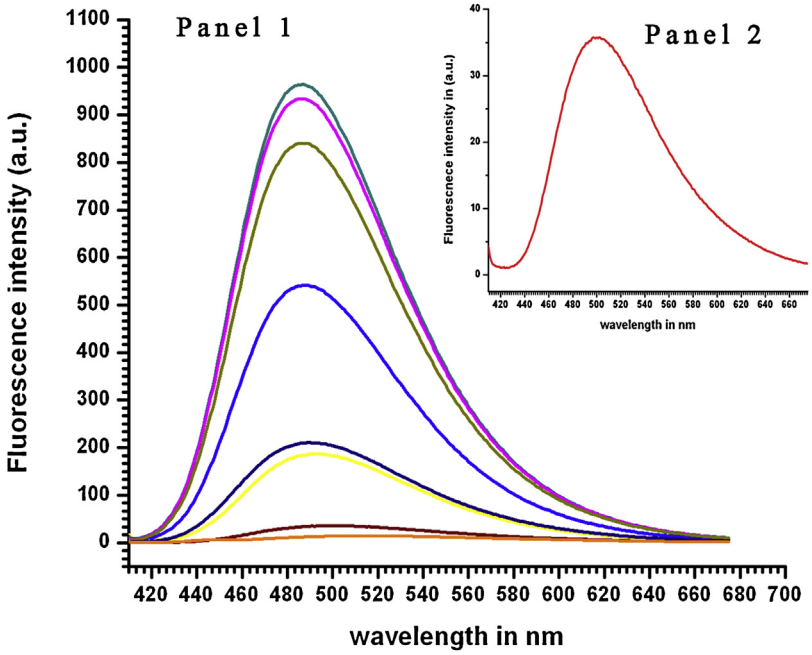

Fig. 7. Panel 1: Bis–ANS fluorescence (10 μM) spectra for LdCyp (4 μM) incubated with various GdmCl concentrations, panel 1: (a) ( ) 4 μM LdCyp + 0.2 M GdmCl (b) ( ) 4 μM LdCyp + 0.7 M GdmCl (c) ( ) 4 μM LdCyp + 1.0 M GdmCl (d) ( ) 4 μM LdCyp + 1.2 M GdmCl (e) ( ) 4 μM LdCyp + 1.4 M GdmCl, (f) ( ) 4 μM LdCyp + 1.5 M GdmCl (g) ( ) 4 μM LdCyp + 1.9 M GdmCl (h) ( ) 4 μM LdCyp + 3.0 M GdmCl. Panel 2: The native spectra ( ) 4 μM LdCyp is shown in Panel 2.

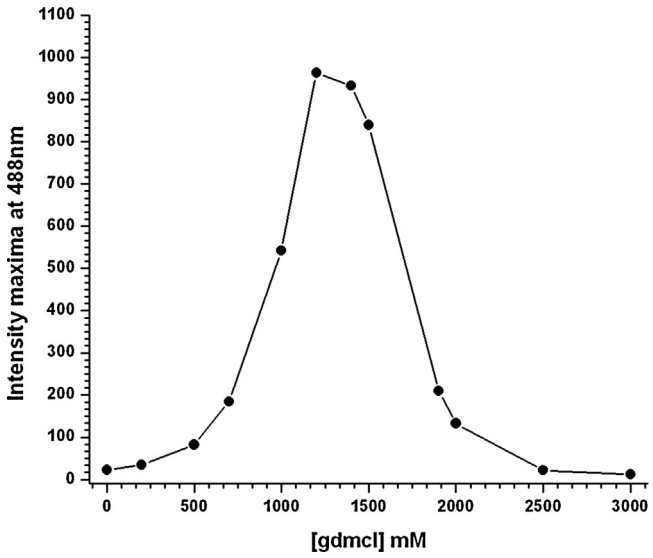

Fig. 8. Plot of Bis–ANS fluorescence (10 μM) intensity maximum in black circles (•) at maximum blue shifted wavelength of 488 nm plotted as a function of GdmCl concentration, with maximum peak intensity obtained for protein sample (4 μM) incubated with 1.2 M GdmCl.

GdmCl after which the change is not significant (see Table 2) at higher denaturant concentrations suggesting maximum exposure of the said tryptophan to occur by 1.4 M. The dynamic character of the quenching was also confirmed by repeating the experiment at a higher temperature at 45 °C, which gave Stern–Volmer coefficients different from those at 25 °C (Supplementary Information, Fig. S5 and Table S2).

Table 2
Dependence of K_{SV} values on denaturant concentrations.

Denaturant concentration in M	K_{SV} values in M^{-1}
0.0	7.64 ± 0.23
0.2	8.84 ± 0.87
1.2	11.65 ± 0.94
1.4	13.18 ± 1.05
3.0	12.87 ± 1.11

The K_{SV} values in this table were calculated using the Stern–Volmer equation, Eq. (1) by linear least square fitting.

3.4. Differential scanning calorimetry

In order to thermally characterize the intermediate states, differential scanning calorimetry was performed with the native protein and also in the presence of different denaturant concentrations. For the native protein reversibility was observed only till 54.6 °C, despite being tested on a wide range of buffering conditions and scan rates. The DSC thermogram of native LdCyp could be best fitted to a non-two state process with two T_m's at 49.6 °C and 54.6 °C. 'Different scan rates (at 20 and 60 °C/h) did not significantly alter the position of the peak in Cp(T), the shape of the curve in the thermogram or the value of the two T_m's (Supplementary information. Figs. S6, S7 and Table S3), confirming that the shoulder observed in the theremograms were unlikely due to kinetic effects.' The apparent ΔH of the transitions were 100 kcal mol^{-1} and 117 kcal mol^{-1}, respectively. DSC measurements under identical conditions with the addition of 0.2 M GdmCl gave a similar thermogram, but with reduction in both T_m's by about 5 °C (44.9 and 50.6 °C) and a concomitant decrease in their ΔH (75.2 and 104.7 kcal mol^{-1}), respectively. Although

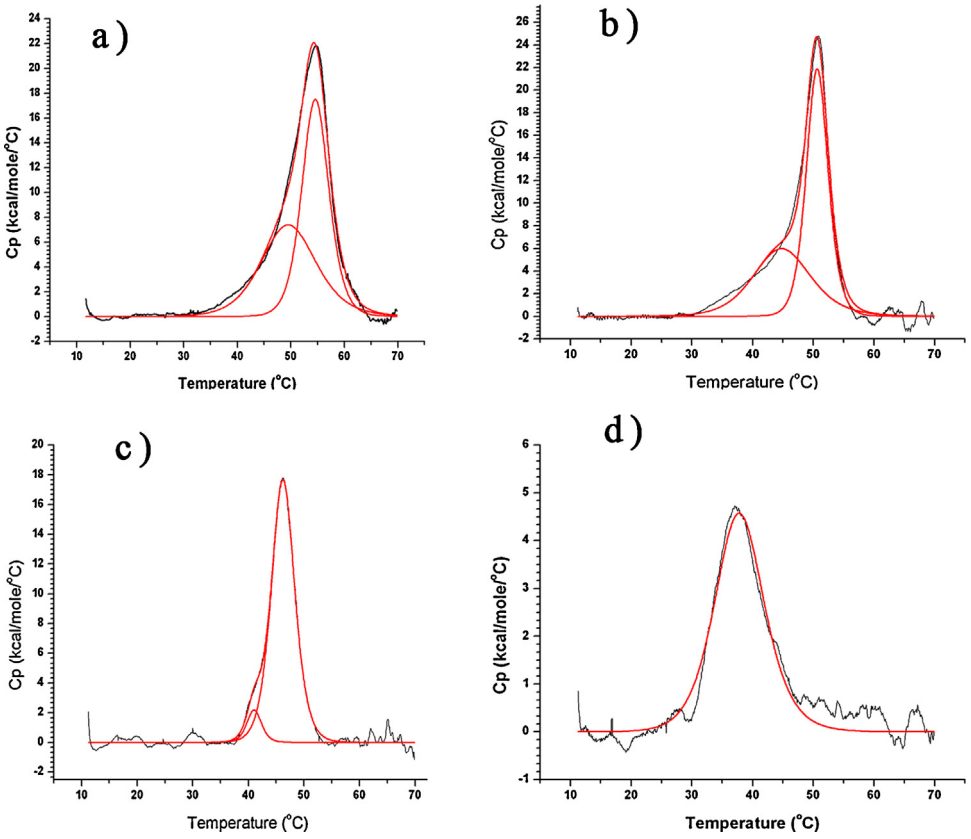

Fig. 9. Thermal characterization of the intermediate states of LdCyp through DSC (a) 10 μM LdCyp, (b) 10 μM LdCyp + 0.2 M GdmCl, (c) 10 μM LdCyp + 0.6 M GdmCl, (d) 10 μM LdCyp + 1.0 M GdmCl, two step (two T_m values) to a single step (one T_m value) transition. The black solid line (▬) corresponds to the experimental data points while the solid red line (▬) are the fitted lines. (For interpretation of the references to color in this figure legend, the reader is referred to the web version of the article.)

Table 3
The fraction of native contacts conserved between the residues constituting the helices (H1, H2) and the remaining residues in the core, averaged over 50 ns for each MD simulation run at 310, 400 and 450 K, respectively. The standard deviation is given in parentheses. The fractional conservation of secondary structural content with respect to the native crystal structure is also given.

Temperature (K)	Fraction of native contacts conserved		Fraction of secondary structural content		
	Helix H1 – core	Helix H2 – core	Helix H1	Helix H2	Beta strands
310	0.73(0.16)	0.65(0.23)	0.92(0.02)	0.89(0.01)	0.97(0.02)
400	0.65(0.18)	0.47(0.29)	0.92(0.03)	0.60(0.27)	0.86(0.05)
450	0.48(0.21)	0.37(0.30)	0.70(0.28)	0.51(0.29)	0.81(0.12)

the non-two state character (with two T_m's) of the thermogram was still maintained at 0.6 M GdmCl, yet there was a significant reduction in the apparent enthalpy ΔH of the first transition (T_m = 41.0 °C, ΔH = 7.7 kcal mol^{-1}) relative to the second (T_m = 46.3, ΔH = 98 kcal mol^{-1}), with further decrease in the two T_m's. At 1.0 M GdmCl a single transition was observed at T_m = 37.9 °C and ΔH = 49.5 kcal mol^{-1} (Fig. 9). At still higher concentrations (1.4 M and above) no statistically significant peak was observed in the DSC measurement most probably indicating the initiation of the molten globule like intermediate, mentioned previously.

3.5. Molecular dynamics simulations

LdCyp consists of a single extended hydrophobic core, whose constituent residues are primarily contributed by the beta strands composing the barrel (see Fig. 1), the two helices (H1, H2) and a few from surrounding loops. Initially, three sets of residues were constructed; S1: residues constituting helix H1; S2: residues constituting helix H2 and S3: residues of the hydrophobic core excluding those from helices H1, H2 contributed by beta strands and loops (Supplementary Information, Table S4). To study the disposition of the helices with respect to the barrel (upon raising temperature in an MD simulation; see Section 2.7), the contacts (see Supplementary Table S5) between S1–S3 and S2–S3 were first calculated from the crystal structure (2HAQ). 4.0 Å was considered to be the distance cutoff for two atoms to be in contact. The fractional conservation of these native contacts (between the helices and the remaining residues of the core) were then estimated for all snapshots and averaged over 50 ns for each simulation run at temperatures 310, 400 and 450 K (Table 3). In addition (average) fractional conservation of secondary structural content (with respect to the native crystal structure) was also calculated for each simulation (50 ns).

On an average, about 0.65–0.75 of the native contacts between helices and core, were conserved in the simulation at 310 K. However, helix H2 appeared to be relatively loosely bound to the core compared to H1, with a sharper decline in the conserved fraction upon elevation of temperature to 400 K (H1 – 0.65(0.18); H2 – 0.47(0.29)). At 450 K, 0.48, 0.37 of the native contacts were conserved for H1, H2 respectively. Again, H2 also exhibited an increased tendency to unwind as only 40% of its constituent residues (as found in the crystal structure) retained their helical conformation even by 400 K. In general, the strands constituting the barrel appear to have greater stability (0.81 secondary structural content conserved, Table 3), in contrast to both the helices. Thus, the simulations appeared to indicate the tendency of both helices to gradually unwind and adopt non-native geometries with respect to the core, quite early in the unfolding process.

4. Conclusion

The work reported in this paper characterizes the equilibrium unfolding of cyclophilin mediated by the denaturant GdmCl. Initial evidence for the existence of intermediate states appears with regard to the non-superposition of the unfolding curves monitored by fluorescence and CD. Analysis of the near and far UV CD spectra indicates the pronounced disruption of the native tertiary contacts at 1.2 M GdmCl while conserving significant fraction of the native secondary structural content, characteristic of a molten globule [23–35]. This was further confirmed by hydrophobic dye-binding studies utilizing bis-ANS where a prominent peak was observed at 1.2 M GdmCl. Thermal characterization of the protein incubated with 0.2, 0.6 and 1.0 M of GdmCl by DSC exhibited a gradual shift from a two (involving two T_m's) to a single step transition (with a unique T_m).

Examination of the native crystal structure and data from MD simulations leads us to hypothesize that the possible equilibrium intermediate could involve disjuncture of the helices from their native geometry with respect to the barrel/core during initial stages of the unfolding process.

Authors' contributions

Dipak Dasgupta and Rahul Banerjee conceived the experiments, Sourav Roy performed the experiments. Dhananjay Bhattacharyya gave guidance and Sankar Basu participated in Molecular Dynamics Simulations. Rahul Banerjee, Dipak Dasgupta and Sourav Roy wrote the manuscript.

Conflict of interest

None declared.

Acknowledgements

The authors thank Prof. Krishnananda Chattopadhayay (Indian Institute of Chemical Biology) and Dr. Amrita Dasgupta (National Centre for Biological Sciences) for providing valuable suggestions and comments. This work was supported by the intramural grants from Department of Atomic Energy, Government of India (Projects of SINP:- MSACR [XII-R&D-SIN-5.04-0102] and BARD -[XII-R&D-SIN-5.04-0103]).

Appendix A. Supplementary data

Supplementary data associated with this article can be found, in the online version, at http://dx.doi.org/10.1016/j.ijbiomac.2014.05.063.

References

[1] Ashutosh, S. Sundar, N. Goyal, J. Infect. Dis. 56 (2007) 143–153, http://dx.doi.org/10.1099/jmm.0.46841-0.
[2] D. Sereno, P. Holzmuller, J.L. Lemesre, Acta Trop. 74 (2000) 25–31.
[3] J. Bua, L.E. Fichera, A.G. Fuchs, M. Potenza, M. Dubin, R.O. Wenger, G. Morretti, C.M. Scabone, A.M. Ruiz, Parasitology 135 (2008) 217–228.
[4] M.E. Perkins, T.W. Wu, S.M. Le Blancq, Antimicrob. Agents Chemother. 42 (1998) 843–848.
[5] P. Wang, J. Heitman, Genome Biol. 6 (2005) 226.
[6] H. Du, L. Guo, F. Fang, D. Chen, A.A. Sosunov, G.M. McKhann, Y. Yan, C. Wang, H. Zhang, J.D. Molkentin, F.J. Gunn-Moore, J.P. Vonsattel, O. Arancio, J.X. Chen, S.D. Yan, Nat. Med. 14 (2008) 1097–1105.
[7] Z. Keckesova, L.M. Ylinen, G.J. Towers, J. Virol. 80 (2006) 4683–4690.

[8] J. Kallen, V. Mikol, P. Taylor, M.D. Walkinshaw, J. Mol. Biol. 283 (1998) 435–449.
[9] H. Ke, J. Mol. Biol. 228 (1992) 539–550.
[10] V. Venugopal, B. Sen, A.K. Datta, R. Banerjee, Acta Crystallogr. F 63 (2007) 60–64.
[11] D. Mitra, S. Mukherjee, A.K. Das, FEBS Lett. 580 (2006) 6846–6860.
[12] D.A. Pearlman, D.A. Case, J.W. Caldwell, W.S. Ross, T.E. Cheatham, S. De Bolt, D. Ferguson, G. Siebel, P. Kollman, Comput. Phys. Commun. 91 (1995) 1–41.
[13] J.C. Phillips, R. Braun, W. Wang, J. Gumbart, E. Tajkhorshid, E. Villa, C. Chipot, R.D. Skeel, L. Kale, K. Schulten, J. Comput. Chem. 26 (16) (2005) 1781–1802.
[14] J.P. Ryckaert, G. Ciccotti, H.J.C. Berendsen, J. Comput. Phys. 23 (1977)327–341.
[15] W. Humphrey, A. Dalke, K. Schulten, J. Mol. Graph. 14 (1996) 33–38 http://www.ks.uiuc.edu/Research/vmd/
[16] D. Frishman, P. Argos, Proteins: Struct. Funct. Genet. 23 (1995) 566–579.
[17] A.H. Wani, J.B. Udgaonkar, J. Mol. Biol. 387 (2009) 348–362.
[18] A.K. Mandal, S. Samaddar, R. Banerjee, S. Lahiri, A. Bhattacharyya, S. Roy, J. Biol. Chem. 278 (2003) 36077–36084.
[19] R.F. Latypov, H. Cheng, N.A. Roder, J. Zhang, H. Roder, J. Mol. Biol. 357 (2006) 1009–1025.
[20] S. Lindhoud, A.H. Westphal, J.W. Borst, C.R.M. van Mierlo, PLoS ONE 7 (10) (2012), http://dx.doi.org/10.1371/journal.pone.0045746.
[21] L. Zhu, Y.X. Fan, J.M. Zhou, Biochim. Biophys. Acta 1544 (2001) 320–332.
[22] G.V. Semisotnov, N.A. Rodionova, O.I. Razgulyaev, V.N. Uversky, A.F. Gripas, R.I. Gilmanshin, Biopolymers 31 (1991) 119–128.
[23] A.L. Fink, L.J. Calciano, Y. Goto, T. Kurotsu, D.R. Palleros, Biochemistry 33 (1994) 12504–12511.
[24] B.K. Das, T. Bhattacharyya, S. Roy, Biochemistry 34 (1995) 5242–5247.
[25] R.L. Baldwin, C. Frieden, G.D. Rose, Proteins 78 (2010) 2725–2737.
[26] D. Barrick, R.L. Baldwin, Protein Sci. 2 (1993) 869–876.
[27] A. Iram, T. Alam, J.M. Khan, T.A. Khan, R.H. Khan, A. Naeem, PLoS ONE 8 (8) (2013), http://dx.doi.org/10.1371/journal.pone.0072075.
[28] K. Kuwajima, Proteins 6 (1989) 87–103.
[29] K. Kuwajima, FASEB J. 10 (1996) 102–109.
[30] M. Ferrer, G. Barany, C. Woodward, Nat. Struct. Biol. 2 (1995) 211–217.
[31] H. Christensen, R.H. Pain, Eur. Biophys. J. 19 (1991) 221–229.
[32] S.H. Park, J. Biochem. Mol. Biol. 37 (2004) 676–683.
[33] S. Sheshadri, G.M. Lingaraju, R. Vardarajan, Protein Sci. 8 (1999) 1689–1695.
[34] O.B. Ptitsyn, V.N. Uversky, FEBS Lett. 341 (1994) 15–18.
[35] S.K. Jha, J.B. Udgaonkar, Proc. Natl. Acad. Sci. U.S.A. 106 (2009) 12289–12294.